

## A mechanochemical model of striae distensae

Stephen J. Gilmore<sup>a</sup>, Benjamin L. Vaughan Jr.<sup>b,\*</sup>, Anotida Madzvamuse<sup>c</sup>, Philip K. Maini<sup>b,d</sup>

<sup>a</sup> *Dermatology Research Centre, University of Queensland, School of Medicine, Princess Alexandra Hospital, Brisbane, Australia*

<sup>b</sup> *Centre for Mathematical Biology, Mathematical Institute, University of Oxford, UK*

<sup>c</sup> *Department of Mathematics, University of Sussex, UK*

<sup>d</sup> *Oxford Centre for Integrative Systems Biology, Department of Biochemistry, University of Oxford, UK*

### ARTICLE INFO

#### Article history:

Received 6 October 2011

Received in revised form 28 June 2012

Accepted 29 June 2012

Available online 14 July 2012

#### Keywords:

Stretch marks

Mathematical modelling

Numerical simulation

### ABSTRACT

Striae distensae, otherwise known as stretch marks, are common skin lesions found in a variety of clinical settings. They occur frequently during adolescence or pregnancy where there is rapid tissue expansion and in clinical situations associated with corticosteroid excess. Heralding their onset is the appearance of parallel inflammatory streaks aligned perpendicular to the direction of skin tension. Despite a considerable amount of investigative research, the pathogenesis of striae remains obscure. The interpretation of histologic samples – the major investigative tool – demonstrates an association between dermal lymphocytic inflammation, elastolysis, and a scarring response. Yet the primary causal factor in their aetiology is mechanical; either skin stretching due to underlying tissue expansion or, less frequently, a compromised dermis affected by normal loads. In this paper, we investigate the pathogenesis of striae by addressing the coupling between mechanical forces and dermal pathology. We develop a mathematical model that incorporates the mechanical properties of cutaneous fibroblasts and dermal extracellular matrix. By using linear stability analysis and numerical simulations of our governing nonlinear equations, we show that this quantitative approach may provide a realistic framework that may account for the initiating events.

© 2012 Elsevier Inc. All rights reserved.

### 1. Introduction

Striae distensae, commonly known as stretch marks, are benign skin lesions associated with considerable cosmetic morbidity. Heralding their onset is the appearance of parallel inflammatory streaks aligned perpendicular to the direction of skin tension. The evolution of striae is characterised by at least two phases: an initial inflammatory phase known as striae rubra and a later, chronic phase known as striae alba [1]. Striae may occur in a wide variety of clinical settings but most commonly develop initially in either adolescence [2] or pregnancy [3]. Striae may also occur in conditions where the dermis is abnormal: Cushing's syndrome [4], prolonged application of topical steroids [5], or Marfan's syndrome [4] are examples. Finally, striae may develop in association with changes to body habitus such as weight loss [6], cachexia [7], obesity [8], or body-building.

Despite their ubiquity and considerable investigation into their origins, the pathogenesis of striae distensae remains unknown. Genetic factors are likely to be important since striae have been ob-

served in monozygotic twins [9]. Much emphasis has been placed on the effects of skin stretching in the pathogenesis of striae [10] since the lesions are found to be aligned perpendicular to the direction of skin tension. Some investigators have suggested that mechanical rupture of dermal components is an important initiating event. However, there is some debate about the relative importance of skin stretching in the aetiology of striae: one group could not find any relationship between striae and the increase in abdominal girth among pregnant females [11] and it has been noted that striae are rare over the extensor surfaces of joints (regions of skin over a joint that is stretched when the joint is flexed) where the skin is subject to physiologic stretching [12]. Less controversy exists regarding the possible role of glucocorticoids in the pathogenesis of striae. This is largely due to the known associations between alterations to hormonal status observed in pregnancy, weight changes, and adolescence on one hand and the more obvious effects of hormonal changes observed in Cushing's syndrome and topical steroid application on the other. In addition, the catabolic effect of both adrenocorticotropic hormone (ACTH) and cortisol are well known. These hormones may modulate fibroblast activity directly leading to reduced mucopolysaccharide secretion, possible changes to elastic fibres, and reduced collagen via either reduced production or increased collagenase secretion or both. Finally, increased levels of steroid hormones and their metabolites have been found in patients exhibiting striae [13].

\* Corresponding author. Present address: Department of Mathematical Sciences, University of Cincinnati, Cincinnati, Ohio, USA.

E-mail addresses: [s.gilmore1@uq.edu.au](mailto:s.gilmore1@uq.edu.au) (S.J. Gilmore), [vaughabn@ucmail.uc.edu](mailto:vaughabn@ucmail.uc.edu) (B.L. Vaughan Jr.), [a.madzvamuse@sussex.ac.uk](mailto:a.madzvamuse@sussex.ac.uk) (A. Madzvamuse), [maini@maths.ox.ac.uk](mailto:maini@maths.ox.ac.uk) (P.K. Maini).

From the pathologic perspective, the earliest changes are sub-clinical and are only detectable by electron microscopy. These changes involve mast cell degranulation (the release histamine along with other molecules from granules in the mast cell's cytoplasm into the extracellular space) and the presence of activated macrophages in association with mid-dermal elastolysis [14]. While mast cell activation has been reported in association with elastolysis in actinically affected skin (pigmentary changes and elastolysis secondary to chronic UV exposure), anetoderma (circumscribed areas of slack skin due to loss of dermal elastin) has been reported in skin affected by mastocytosis. These findings support the concept that the release of enzymes, possibly elastases (enzymes that are capable of degrading the elastin molecule within the dermis), from mast cells plays a very early and important role in the pathogenesis of striae [14]. When lesions initially become visible, collagen bundles begin to show structural alterations, fibroblasts become prominent, and mast cells are absent [14].

On light microscopy, the earliest changes in striae rubra involve dermal oedema, perivascular lymphocyte cuffing (the appearance of lymphocytes in the surrounding small blood vessels within the dermis), and an associated increase in the glycosaminoglycan content of the dermis [15]. Examination of early lesions shows fine elastic fibres predominating throughout the dermis in association with thick and tortuous fibres toward the periphery [16]. An integral component of elastic fibres, fibrillin microfibrils, are found to be reduced in striae rubra [17]. In contrast to early inflammatory lesions, striae alba are characterised by epidermal atrophy, loss of appendages, and a densely packed region of thin eosinophilic collagen bundles aligned horizontal to the surface. Later stage lesions are thus indistinguishable, from the perspective of light microscopy, from a dermal scar.

A number of studies suggest that fibroblasts play a key role in the pathogenesis of striae. Compared with normal fibroblasts, expression of fibronectin and both type I and III procollagen were found to be significantly reduced in fibroblasts from striae, suggesting that there exist fundamental aberrations of fibroblast metabolism in striae distensae [18]. From a bio-mechanical perspective, ex-vivo fibroblasts from patients with early striae distensae were found to exhibit high levels of alpha-smooth muscle actin and were able to generate higher contractile forces in comparison with fibroblasts from later stage striae [19].

Taken together, the foregoing discussion suggests at least two major factors play important roles in the aetiology of striae distensae: mechanical stretching of the skin and pre-existing dermal pathology. The relative effects of these factors are unknown. For example, it is unknown to what extent steroid hormones in pregnancy or adolescence may pre-condition the skin such that it may be predisposed to developing striae when subjected to stretching.

In this paper we develop a mathematical model that attempts to capture early changes in striae distensae development. We are encouraged by the success of similar models used to describe wound healing [20] and earlier contact guidance models of striae by Murray [21] and Hariharan [22] and we are motivated by the ability of mathematical models to incorporate the postulated relevant elements of early striae development including fibroblast contractility, fibroblast motility and remodelling of the extra-cellular matrix. Our model allows us to quantify the degree of mechanical stretching (given by a single parameter) and dermal stiffness (given by an independent parameter) so that we are able to explore the relevant contributions of skin stretching and glucocorticoid-affected skin [23,24]. Finally, as a model of pattern formation in the skin, we are able to investigate how microscopic events may lead to macroscopic patterns.

The remainder of this paper is organised as follows: Section 2 describes the derivation of our model and a non-dimensionalisation of our governing equations. In Section 3, we perform a linear

stability analysis and investigate mode selection. Section 4 describes our numerical results of the full nonlinear model. We conclude this paper in Section 5 with a discussion of our results and the implications for pathogenesis.

## 2. Model description

Our model is based on the simple assumption that in the pre-clinical phase of striae development there exists spatial inhomogeneity in the density of one or more constituents of the dermis. We thus focus on its two most important components: fibroblasts and the extracellular matrix (ECM). Fibroblasts are spindle-shaped cells embedded within the ECM; they play an essential role in dermal homeostasis, wound healing, and recently have been shown to express a Hox code that accounts for the regional specificity of the epidermal phenotype [25]. Proteoglycans and mucopolysaccharides constitute the ECM. While collagen gives the skin its tensile strength, the proteoglycans and mucopolysaccharides are gel-like substances that trap water, thus facilitating molecular diffusion and cell transport.

Since striae are frequently observed to align in a direction perpendicular to the direction of skin tension, they are found to develop as parallel inflammatory streaks in the skin. Hence, without loss of generality, we can reduce a potential two-dimensional problem to a one-dimensional problem since the patterning is translationally invariant in the direction perpendicular to the direction of skin tension. We thus consider a one-dimensional model, defined on a periodic domain, similar to the model developed by Oster et al. [26] and modified by Vaughan, Jr. et al. [27] where the skin is treated as a visco-elastic medium. The model derived below and the model in Vaughan, Jr. et al. [27] generalise the model discussed in Oster et al. [26] and Murray [21] by keeping the inertial terms and writing the governing equations in the material frame of reference. This derivation keeps the nonlinear terms that arise from transformation from spatial to material frames of reference in the spatial derivatives, which increases the range of parameters where the solution evolves to a bounded steady state [27].

The model consists of conservation equations for the fibroblast cell density,  $\hat{c}$ , and the ECM density,  $\hat{\rho}$ , in a deformed frame of reference coupled through a force balance equation governing the mechanical interaction of the fibroblasts with the ECM, which is defined in the undeformed (reference) frame. In this formulation, we will transform the equations governing the cell and ECM densities from the deformed frame to the reference frame, which will simplify the methods used to solve this model numerically. Note that variables with a hat denote a variable in the deformed frame of reference and variables without a hat are defined in the reference frame.

The stress tensor,  $\sigma$ , satisfies the force balance equation in the reference frame,

$$\rho_0 \frac{\partial^2 u}{\partial t^2} = \frac{\partial}{\partial x} (\sigma + \tau(\hat{c}, \hat{\rho})) + \rho_0 F, \quad (1)$$

where  $u$  is the material displacement,  $\tau(\hat{c}, \hat{\rho})$  is the traction due to cell-ECM interactions and depends on the cell and ECM densities in the deformed frame of reference,  $\rho_0$  is the ECM density in the reference frame, and  $F$  is an external body force. We follow the Oster-Murray-Harris model [26] and treat the ECM as a linear, isotropic, visco-elastic material. Hence, the stress tensor in one dimension is

$$\sigma = A \frac{\partial^2 u}{\partial t \partial x} + B \frac{\partial u}{\partial x}. \quad (2)$$

Here,  $A = \mu_1 + \mu_2$ , where  $\mu_1$  and  $\mu_2$  are the shear and bulk viscosities of the ECM, respectively, and

$$B = E \frac{(1 - \nu)}{(1 + \nu)(1 - 2\nu)},$$

where  $E$  is the Young's modulus and  $\nu$  is the Poisson's ratio of the ECM. It is assumed that the ECM material is attached to the subcutaneous fascia by fibrous bands that resist the lateral displacement of the overlying dermis. We model this attachment as a linear spring and the body force in the force balance equation, (1), is

$$F = -su, \quad (3)$$

where  $s$  is a positive spring constant.

We model the traction exerted by the cell-matrix interactions in the deformed frame of reference as

$$\tau(\hat{c}, \hat{\rho}) = \tau_0 \frac{\hat{c}}{1 + \lambda \hat{c}^2} \left( \hat{\rho} + \beta_0 \frac{\partial^2 \hat{\rho}}{\partial \hat{x}^2} \right), \quad (4)$$

where  $\tau_0$  is the traction strength,  $\lambda$  is a constant that accounts, in a phenomenological way, for contact inhibition,  $\beta_0$  is the strength of the long-range traction that arises from the fibrous nature of the ECM, which can extend the range of the traction force exerted by the fibroblasts, and  $\partial/\partial \hat{x}$  is the spatial derivative in the deformed frame of reference.

We assume that there is no production or degradation of the ECM, so we can relate the ECM density in the deformed frame to the ECM density in the reference frame using the relation  $\rho_0 = J\hat{\rho}$ , where  $J = 1 + \partial u/\partial x$  is the Jacobian of the deformation gradient and  $\rho_0$  is a constant. Likewise, we transform the cell density from the deformed frame to the reference frame using the same relation,  $c = J\hat{c}$ . Here,  $c$  is not assumed to be constant since we will allow for the movement of cells by diffusion.

We transform the derivatives in the long-range traction force into the reference frame by taking the derivative of the definition of the displacement,  $u(x, t) = \hat{x}(x, t) - x$ , with respect to the spatial coordinate in the reference frame, to obtain

$$\frac{\partial}{\partial \hat{x}} = \frac{1}{1 + \partial u/\partial x} \frac{\partial}{\partial x}. \quad (5)$$

Hence, the traction force in the reference frame is

$$\begin{aligned} \tau(c, \partial u/\partial x) &= \tau_0 \frac{c \rho_0}{(1 + \partial u/\partial x)^2 + \lambda c^2} \\ &\times \left( 1 + \beta_0 \frac{\partial}{\partial x} \left( \frac{1}{1 + \partial u/\partial x} \frac{\partial}{\partial x} \left( \frac{1}{1 + \partial u/\partial x} \right) \right) \right). \end{aligned} \quad (6)$$

See Appendix A for the details of the derivation of this term.

Inserting (2) and (6) into (1), the resulting force balance equation in one dimension is

$$\rho_0 \frac{\partial^2 u}{\partial t^2} = \frac{\partial}{\partial x} \left[ A \frac{\partial^2 u}{\partial x \partial t} + B \frac{\partial u}{\partial x} + \tau \left( c, \frac{\partial u}{\partial x} \right) \right] - s \rho_0 u = 0. \quad (7)$$

It is assumed that fibroblasts move randomly and are advected with the medium. Thus the governing equation for the cell density,  $\hat{c}$ , in the deformed frame of reference is

$$\frac{\partial \hat{c}}{\partial \hat{t}} + \frac{\partial}{\partial \hat{x}} (\hat{c} v) = D \frac{\partial^2 \hat{c}}{\partial \hat{x}^2}, \quad (8)$$

where  $v = \partial u/\partial t$  is the velocity of the medium,  $D$  is the diffusion coefficient and  $\hat{t}$  is time in the deformed frame. Relating the cell density in the deformed configuration,  $\hat{c}$ , with the cell density in the initial configuration,  $c$ , using the relation  $c = J^{-1} \hat{c}$  and the change in the spatial derivative, (5), and the change in the temporal derivatives due to the change in frame,

$$\frac{\partial}{\partial t} = \frac{\partial}{\partial \hat{t}} + v \frac{\partial}{\partial \hat{x}}, \quad (9)$$

we obtain

$$\frac{\partial c}{\partial t} = D \frac{\partial}{\partial x} \left[ \frac{1}{1 + \partial u/\partial x} \frac{\partial}{\partial x} \left( \frac{c}{1 + \partial u/\partial x} \right) \right]. \quad (10)$$

Next, we non-dimensionalise Eqs. (10) and (7) using the relations:

$$\begin{aligned} x^* &= \frac{x}{L}, \quad t^* = \frac{t}{T}, \quad c^* = \frac{c}{c_0}, \quad u^* = \frac{u}{L}, \\ \lambda^* &= \lambda c_0^2, \quad \alpha^* = \frac{1}{s T^2}, \quad a^* = \frac{A}{L^2 T s \rho_0}, \quad b^* = \frac{B}{L^2 s \rho_0}, \\ d^* &= \frac{D T}{L^2}, \quad \tau^* = \frac{\tau_0 c_0}{L^2 s}, \quad \beta^* = \frac{\beta_0}{L^2}, \end{aligned} \quad (11)$$

where  $L$  is the characteristic length scale and  $T$  is the characteristic time scale. The non-dimensionalised equations, after dropping the stars, are:

$$\frac{\partial c}{\partial t} = d \frac{\partial}{\partial x} \left[ \frac{1}{1 + \partial u/\partial x} \frac{\partial}{\partial x} \left( \frac{c}{1 + \partial u/\partial x} \right) \right] \quad (12)$$

and

$$\begin{aligned} \alpha \frac{\partial^2 u}{\partial t^2} &= a \frac{\partial^3 u}{\partial x^2 \partial t} + b \frac{\partial^2 u}{\partial x^2} \\ &+ \tau \frac{\partial}{\partial x} \left[ \frac{c}{(1 + \partial u/\partial x)^2 + \lambda c^2} \left( 1 + \beta \frac{\partial}{\partial x} \left[ \frac{1}{1 + \partial u/\partial x} \frac{\partial}{\partial x} \left( \frac{1}{1 + \partial u/\partial x} \right) \right] \right) \right] - u. \end{aligned} \quad (13)$$

Note that we generalise the Oster–Murray–Harris model by keeping the inertial term,  $\alpha \partial^2 u/\partial t^2$ . Even though the  $\alpha$  term is small for physically relevant parameters, the acceleration of the medium,  $\partial^2 u/\partial t^2$ , can be large in the numerical simulations and it would not be appropriate to neglect this term for all time.

The above equations for the dimensionless fibroblast density,  $c$ , and the material displacement,  $u$ , are coupled with appropriate boundary conditions. Since striae occur as parallel lines and are translationally invariant in the transverse direction, we assume in this paper that the solution is periodic in space and, hence, we enforce periodic boundary conditions on the ends of the domain.

### 3. Linear analysis

The linearized versions of Eqs. (12) and (13) around the normalised steady state  $c = 1$  and  $u = 0$  are

$$\frac{\partial c}{\partial t} = d \left( \frac{\partial^2 c}{\partial x^2} - \frac{\partial^3 u}{\partial x^3} \right) \quad (14)$$

and

$$\begin{aligned} \alpha \frac{\partial^2 u}{\partial t^2} &= a \frac{\partial^3 u}{\partial x^2 \partial t} + \left( b - 2 \frac{\tau}{(1 + \lambda)^2} \right) \frac{\partial^2 u}{\partial x^2} \\ &+ \frac{\tau(1 - \lambda)}{(1 + \lambda)^2} \frac{\partial c}{\partial x} - \frac{\tau \beta}{1 + \lambda} \frac{\partial^4 u}{\partial x^4} - u = 0. \end{aligned} \quad (15)$$

By defining  $\tau_\lambda = \tau/(1 + \lambda)^2$  and  $\beta_\lambda = \beta(1 + \lambda)$  and looking for solutions of the form

$$\begin{bmatrix} c \\ u \end{bmatrix} = \mathbf{z} e^{\sigma t + i k x}, \quad (16)$$

where  $\mathbf{z}$  is the eigenvector,  $\sigma$  is the linear growth rate, and  $k$  is the spatial wavenumber, we require  $|A| = 0$ , for

$$A = \begin{bmatrix} \sigma + d k^2 & -i d k^3 \\ -i \tau_\lambda (1 - \lambda) k & \alpha \sigma^2 + a k^2 \sigma + B(k^2) \end{bmatrix}, \quad (17)$$

where

$$B(k^2) = \tau_i \beta_i k^4 + (b - 2\tau_i)k^2 + 1. \tag{18}$$

The characteristic equation is

$$\begin{aligned} \alpha\sigma^3 + (a + \alpha d)k^2\sigma^2 + (B(k^2) + \alpha dk^4)\sigma \\ + dk^2(B(k^2) + \tau(1 - \lambda)k^2) \\ = 0. \end{aligned} \tag{19}$$

If we ignore inertial forces ( $\alpha = 0$ ) and cell diffusion ( $d = 0$ ), we recover the characteristic equation for the basic Oster–Murray–Harris model.

If we take the ratio  $\tau_i/b$  as the bifurcation parameter, the real part of  $\sigma$  can become positive in three ways as  $\tau_i/b$ . Applying the Routh–Horwitz conditions to (19),

$$\begin{aligned} B(k^2) + \alpha dk^4 < 0, \\ d \neq 0 \text{ and } B(k^2) + \tau_i(1 - \lambda)k^2 < 0, \end{aligned} \tag{20}$$

or

$$\alpha dk^2(B(k^2) + \tau_i(1 - \lambda)k^2) \geq (a + \alpha d)k^2(B(k^2) + \alpha dk^4)$$

are the conditions necessary for linear instability.

The first case,  $B(k^2) + \alpha dk^4 < 0$ , will occur when

$$\frac{\tau_i}{b} > \frac{1}{2}, \text{ and } [b - 2\tau_i]^2 = 4(\tau_i\beta_i + \alpha d). \tag{21}$$

The critical wavemode in this case is

$$k_c^2 = \sqrt{\frac{1}{\tau_i\beta_i + \alpha d}}. \tag{22}$$

The presence of diffusion has a stabilizing effect in this case by increasing the critical value of  $\tau_i$  required for a bifurcation from

$$\tau_i = \frac{b}{2} + \frac{1}{2}(\beta + \sqrt{\beta(2b + \beta)}), \tag{23}$$

in the original Oster–Murray–Harris model to

$$\tau_i = \frac{b}{2} + \frac{1}{2}(\beta + \sqrt{\beta(2b + \beta) + 4\alpha d}). \tag{24}$$

The second case,  $d \neq 0$  and  $B(k^2) + \tau_i(1 - \lambda)k^2 < 0$ , will occur when

$$\frac{\tau_i}{b} > \frac{1}{1 + \lambda} \text{ and } [b - (1 + \lambda)\tau_i]^2 = 4\tau_i\beta_i. \tag{25}$$

The critical wavemode is

$$k_c^2 = \sqrt{\frac{1}{\tau_i\beta_i}}. \tag{26}$$

Note that this case only arises if there is cell diffusion,  $d \neq 0$ .

The third case will occur when

$$\begin{aligned} \frac{\tau_i}{b} > \frac{1}{2 + \frac{\alpha d}{a}(1 - \lambda)} \text{ and } \left[ b - \left( 2 + \frac{\alpha d}{a}(1 - \lambda) \right) \tau_i \right]^2 \\ = 4(\tau_i\beta_i + d(a + \alpha d)). \end{aligned} \tag{27}$$

The critical wavemode is

$$k_c^2 = \sqrt{\tau_i\beta_i + d(a + \alpha d)}. \tag{28}$$

Note that when  $\lambda \geq 1 + 2a/\alpha d$ , this case never produces a bifurcation as  $\tau_i$  is increased.

If  $\lambda \neq 1$ , diffusion causes the system to be able to reach a bifurcation for different values of critical  $\tau_i$ , which depend on the parameters  $b, \beta, \alpha, a$ , and  $d$ . When  $\lambda = 1$ , the bifurcation conditions in the second case, (25), are reached first for all values of  $b, \beta, \alpha, a$ , and  $d$  and are identical to the bifurcation conditions for the original Oster–Murray–Harris model.

The fixed, dimensional parameter values we use for this system are [28–30,21,31,32]

$$\begin{aligned} A = 10^5 \text{ poise, } D_0 = 10^{-9} \frac{\text{cm}^2}{\text{s}}, \beta = 10^{-2} \text{ cm}^2, \\ s = 10^2 \frac{1}{\text{s}^2}, c_0 = 10^4 \frac{\text{cell}}{\text{cm}^3}, \rho_0 = 10^{-1} \frac{\text{g}}{\text{cm}^3}. \end{aligned} \tag{29}$$

Using the length scale  $L = 1$  cm and the time scale  $T = 10$  s, these correspond to the non-dimensional parameters

$$\alpha = 10^{-4}, a = 10^3, d = 10^{-8}, \beta = 10^{-2}. \tag{30}$$

We set  $\lambda = 1$  and the two parameters,  $b$  and  $\tau$ , are chosen so that the uniform steady state is linearly unstable to small random perturbations. Fig. 1 shows the dispersion relation for the root of (19) with a positive real part for various values of  $\tau$  with  $b = 1.012$  ( $B = 10.12$  dynes/cm<sup>2</sup>). A bifurcation occurs for  $\tau > 2.469$  ( $\tau_0 > 2.469 \times 10^{-5}$  dynes cm<sup>4</sup>/cell mg) where only one root has a positive real part for  $k^2 \neq 0$  and the other two have negative real parts for  $k^2 \neq 0$ .

For  $k^2 = 0$ , the three roots are  $\sigma = 0, \pm i/\sqrt{\alpha}$ . The  $\sigma = 0$  root corresponds to a uniform increase/decrease in the cell density. Since we can scale any perturbations in the total cell density out, we can neglect this root. The  $\sigma = \pm i/\sqrt{\alpha}$  roots correspond to oscillatory translation of the medium. These oscillations do not affect

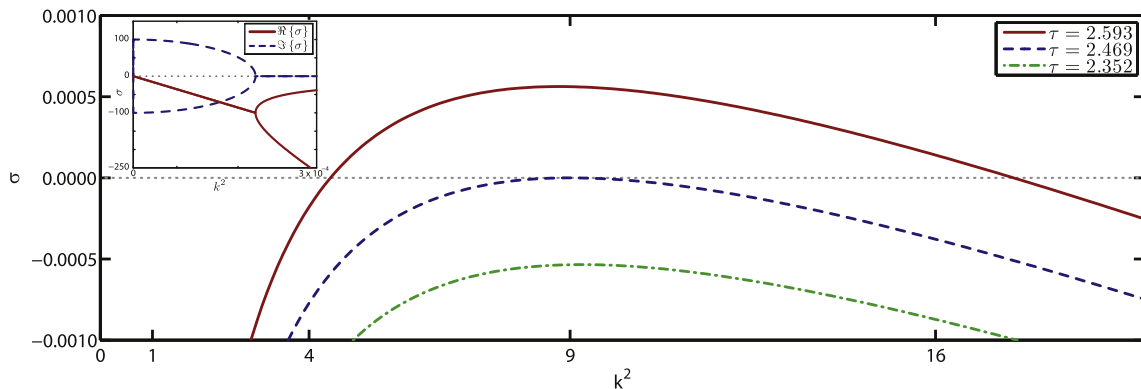


**Fig. 1.** Dispersion relation as the bifurcation parameter  $\tau$  is increased. The other two roots of the characteristic Eq. (19),  $\sigma_2$  and  $\sigma_3$ , are not shown and  $\Re\{\sigma_2, \sigma_3\} \leq 0$ . The roots are real except for a narrow region (shown in the inset),  $0 \leq k^2 \leq 2 \times 10^{-4}$  for  $\tau = 2.5933$ , where the roots are complex with a negative real part. For  $k^2 = 0$ , the root is purely complex.

the cell/ECM densities and do not contribute to the nonlinear dynamics of the system.

For  $k^2 \neq 0$ , the root with a positive real part has a zero imaginary part except for a thin region,  $0 < k^2 < 2 \times 10^{-4}$ . This narrow range of wavemodes are not admissible unless the domain is of sufficient length and are not admissible for biologically relevant domain sizes in this paper.

#### 4. Numerical results

We numerically solve Eqs. (12) and (13) using finite differences in space and the backward Euler method in time. We take the domain to be periodic with length  $2\pi$  cm discretised using a mesh with 300 grid points and a time step of  $\Delta t = 10^{-1}$ . The uniform steady state solution for  $u$  and  $c$  is perturbed using a uniform random function with mean zero and the amplitude of the perturbations are  $10^{-2}$ . The numerical solutions are independent of grid size for grids that are sufficiently refined to resolve the significant spatial frequencies in the problem and are independent of the exact random initial condition subject to a phase shift.

From a biological point of view, we suggest the precursors of clinically evident striae may appear as regions of ECM density that are below the uniform steady state value ( $u = 0$ ,  $\rho = c = 1$ ). Fig. 2 shows the dilation and the ECM density after four days for  $b = 1.012$  ( $B = 10.12$  dynes/cm<sup>2</sup>) and  $\tau = 2.593$  ( $\tau_0 = 2.593 \times 10^{-5}$  dynes cm<sup>4</sup>/cell mg). In the ECM density, we can see the development after four days of regions where there is a significant decrease in density ( $\min \rho \approx 74\% \rho_0$ ). This corresponds to a  $2.6 \times 10^{-2}$  g/cm<sup>3</sup> decrease in ECM density at the minima. The critical wavemode is  $k_c = 3$  and this corresponds to an interlesional distance of approximately 2.09 cm. The above numerical solution is not a steady state solution. There is a second phase of growth that is due to the diffusion of fibroblasts. We can see slow growth

in the displacement and cell/ECM densities at 45 and 90 days. Here, the maximum cell density has increased by a total 2% after 90 days. Any appreciable effect due to this slow growth will occur over a long time frame and since we are interested in the onset of patterns that can become precursors of striae distensae, we will focus on the initial development of patterning.

#### 5. Discussion

We have described in detail a mathematical model proposed to capture the earliest events in the pathogenesis of striae distensae. Motivation for the model is twofold: first, we are interested in exploring the relative contributions of both skin stretching and corticosteroid effects in the pathogenesis of striae; and second, we are interested in the process of pattern formation in striae. Since stretch marks are frequently observed to align perpendicular to the direction of skin tension, it is likely that the effects of tissue forces play an important role in the genesis of striae, and in determining the patterns that form. These considerations naturally lead to a mechanochemical type model.

In this paper, we have reformulated Murray's mechanochemical modelling approach [21] by stating the equations in a common frame of reference. In the limit of small displacements this reduces to the original model, but crucially, the model is now applicable over a much wider range of parameter space and boundary conditions [27]. The work by Hariharan [22] (under the supervision of one of the authors) lists some preliminary results on this problem, but these are significantly extended.

We have shown that an intuitive model incorporating the density of fibroblasts, the density of extracellular matrix, and a force balance equation that accounts for the contractile forces generated by fibroblasts is able to predict, for biologically realistic parameters, periodic solutions for ECM density. In this periodic spatial

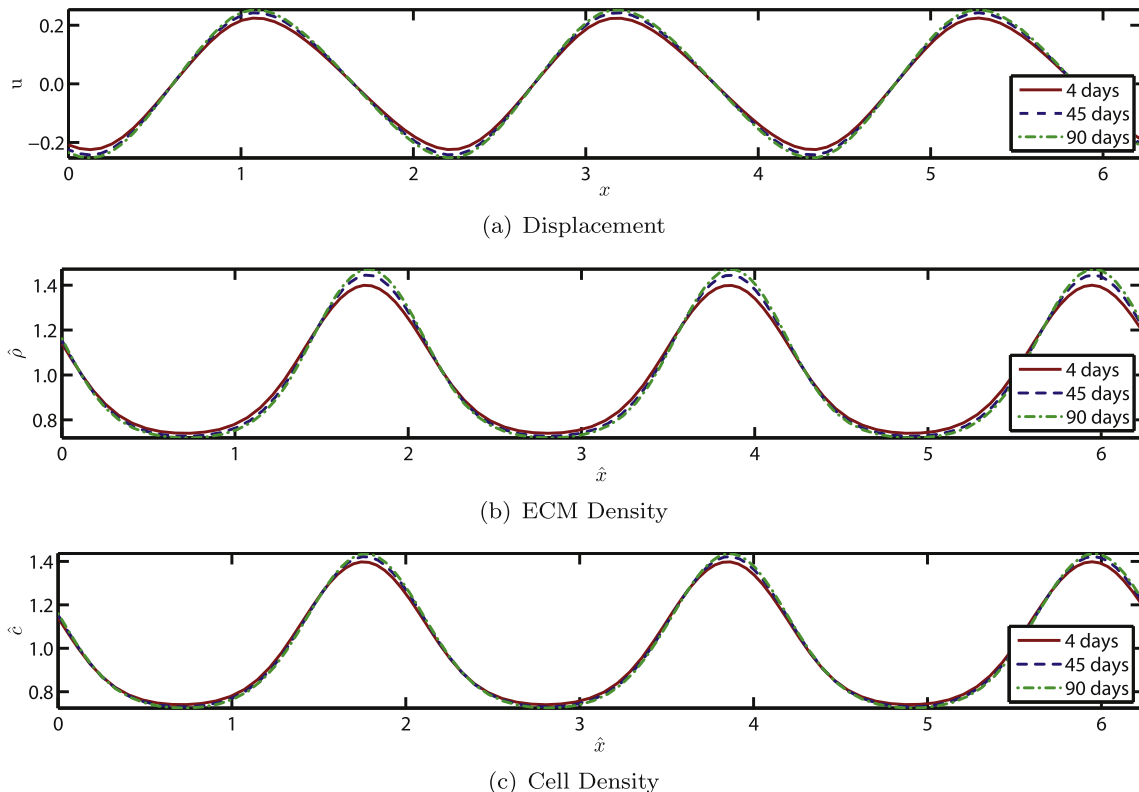


**Fig. 2.** Numerical solution of Eqs. (12) and (13) after 4, 45, and 90 days for  $\hat{b} = 1.012$  and  $\hat{\tau} = 2.593$ . The ECM and cell densities are in the deformed variables in the deformed frame of reference. The minima after four days represent a 26% decrease in ECM density and the interlesional distance is approximately 2.09 cm.

pattern, the precursors of striae are postulated to appear in close proximity to regions of ECM density at their maximal densities.

As discussed in Section 1, an important unresolved issue with regard to the pathogenesis of striae distensae is the relative contributions of skin stretching on one hand, and endocrine factors on the other. While some investigators have suggested that striae may simply result from tissue rupture due to mechanical loads, endocrine changes are present in association with many of the clinical situations in which striae are encountered [12]. In our model, we are able to quantify the degree of stretch imposed on the skin by our parameter  $\tau_0$  (which is a measure of the contractile force exerted by fibroblasts on the surrounding extracellular matrix) since the fibroblasts respond to external mechanical force by opposing that force. Furthermore, we are able to characterize the skin stiffness by adjusting  $B$ , a parameter proportional to the Young's modulus. Since it is recognised that corticosteroid exposure may increase skin extensibility [23,24], we can model the effects of corticosteroid excess by reducing  $B$ . Our results suggest that the uniformity of cutaneous extracellular matrix may be rendered unstable by either increasing  $\tau_0$  or decreasing  $B$ . We obtain solutions that are qualitatively identical via two distinct mechanisms, and these distinct mechanisms correspond to either stretching of the skin or increasing the extensibility of skin. From the clinical perspective, these results suggest that either factor alone can induce striae. For example, in adolescence striae may develop simply as a result of skin stretching (increasing  $\tau_0$ ); abnormal endocrine factors and changes to skin extensibility are not needed. Conversely, the application of potent topical steroids to the skin results in a reduction in the mucopolysaccharide content [33] – and this may account for the increases in skin extensibility reported [24] – with the subsequent development of striae under normal skin tension. Indeed, the skin is not subject to increased stretch in a number of clinical situations where striae distensae arise: cachexia (a wasting syndrome associated with malignancy or chronic infection) and other causes of severe weight loss are two examples where decreased dermal substrate and the resultant increased extensibility of skin may be the sole aetiological factor. Interestingly, of seven patients treated with high dose intravenous corticosteroid for alopecia areata (an autoimmune disease associated with circular patches of hair loss in the scalp) [23] one patient developed striae distensae on the thighs within four days of the infusion. In this study skin extensibility was measured and was shown to increase within hours of the infusion, reaching a maximal extensibility at around four days. In ageing skin it has been reported that there is a decrease in extensibility [34] (corresponding to an increase in  $B$  in our model) and perhaps explaining why striae are only rarely observed to develop in mature adults. Finally, our model is not inconsistent with both increased stretch and dermal changes acting together in the genesis of striae. For example, in pregnancy lesions may arise due to the synergistic effect of both increased skin extensibility on one hand, and the increased mechanical forces acting on the skin secondary to a rapidly distending abdomen on the other.

Striae distensae in the skin often exhibit typical patterns. Although the individual lesions are linear and usually 5–10 cm long, multiple lesions are the norm and are always aligned perpendicular to the axis of skin tension. Striae develop on the back of adolescent males as parallel streaks perpendicular to the direction of vertical growth. Conversely, striae on the breasts in females often have a radial pattern indicating that the lines of tension in the skin in an enlarging breast are circumferential. Although our model is one-dimensional, we are able to predict the existence of periodic solutions that arise parallel to the direction of tension, consistent with the clinical observations noted above. We have shown the dimensional value for the wavelength of our solutions can be adjusted to approximate 1 cm. This result is in good agreement with

the average distance found between striae that are aligned in a parallel arrangement.

Although we have demonstrated that increases in the contractile forces exhibited by fibroblasts or increases to skin extensibility may lead to dermal inhomogeneity of ECM density, we have been unable to provide a definite link between these changes and the mast cell degranulation that is known to be an early event in the pathogenesis of striae. However, it is known that increases in GAG (glycosaminoglycan) density is a very early finding in striae rubra [15], and it is unclear at present whether these changes pre-date, coincide with, or follow the mast cell associated elastolysis. Our model, in predicting periodicity in ECM density along the axis of skin tension, adds weight to the hypothesis that local increases in GAG density (since the GAG is part of the ECM) may precede mast cell degranulation. Since fibroblasts in early striae are known to exhibit aberrant gene expression profiles, one possible pathogenic mechanism is apparent: secreted fibroblast products may exist locally in higher concentrations where the ECM density is higher and thus lead to spatially dependent mast cell recruitment and subsequent elastolysis.

In summary, we present a conceptually simple but mathematically complex model that attempts to account for the earliest events in the pathogenesis of striae distensae. We suggest that the results are sufficiently robust enough to provide evidence for the existence of an important symmetry breaking mechanism that is able to distinguish between two fundamentally different and clinically relevant causes.

#### Acknowledgements

The authors thank Dr. Cameron Hall for his helpful insights. B.L.V. was partially supported by St. John's College, Oxford. P.K.M. was partially supported by a Royal Society Wolfson Research Merit Award.

#### Appendix A. Transformation of the traction force into the material frame of reference

We begin with the traction force exerted by the fibroblasts on the ECM in the spatial frame of reference:

$$\tau(\hat{c}, \hat{\rho}) = \tau_0 \frac{\hat{c}}{1 + \lambda \hat{c}^2} \left( \hat{\rho} + \beta_0 \frac{\partial^2 \hat{\rho}}{\partial \hat{x}^2} \right), \quad (\text{A.1})$$

where the hats designate the spatial frame of reference. We transform  $\hat{c}$  and  $\hat{\rho}$  from the spatial frame to the reference frame using the Jacobian of the deformation gradient,  $J = 1 + \partial u / \partial x$ , to get

$$\hat{c} = \frac{c}{1 + u_x} \quad \text{and} \quad \hat{\rho} = \frac{\rho_0}{1 + u_x}, \quad (\text{A.2})$$

where  $u_x = \partial u / \partial x$ . Substituting (A.2) into (A.1) and simplifying yields the equation

$$\tau_0 \frac{c \rho_0}{(1 + u_x)^2 + \lambda c^2} \left( 1 + \beta \frac{\partial}{\partial \hat{x}^2} \left( \frac{1}{1 + u_x} \right) \right). \quad (\text{A.3})$$

Next, we convert the spatial derivatives to the reference frame using

$$\frac{\partial}{\partial \hat{x}} = \frac{1}{1 + u_x} \frac{\partial}{\partial x}, \quad (\text{A.4})$$

to obtain the traction force in the reference frame:

$$\tau \left( c, \frac{\partial u}{\partial x} \right) = \tau_0 \frac{c \rho_0}{(1 + u_x)^2 + \lambda c^2} \left( 1 + \beta \frac{\partial}{\partial x} \left( \frac{1}{1 + u_x} \frac{\partial}{\partial x} \left( \frac{1}{1 + u_x} \right) \right) \right). \quad (\text{A.5})$$

## References

- [1] P. Zheng, R.M. Lavker, A.M. Kligman, Anatomy of striae, *Brit. J. Dermatol.* 112 (2) (1985) 185.
- [2] H. Herxheimer, Cutaneous striae in normal boys, *Lancet* 265 (6778) (1953) 204.
- [3] J.C. Murray, Pregnancy and the skin, *Dermatol. Clin.* 8 (2) (1990) 327.
- [4] G. Moretti, A. Rebora, M. Guarrera, Striae distensae: how and why they are formed, *Striae Distensae*, Brocades Milan, 1976.
- [5] M.E. Chernosky, J.M. Knox, Atrophic striae after occlusive corticosteroid therapy, *Arch. Dermatol.* 90 (1) (1964) 15.
- [6] A.J. Arem, C.W. Kischer, Analysis of striae, *Plast. Reconstr. Surg.* 65 (1) (1980) 22.
- [7] M. Spraker, E. Garcia-Gonzalez, L. Tamayo, Sclerosing and atrophying conditions, *Pediatr. Dermatol.* (1988) 925.
- [8] W.R. Sisson, Colored striae in adolescent children, *J. Pediatr.* 45 (5) (1954) 520.
- [9] V. Di Lernia, A. Bonci, M. Cattania, G. Bisighini, Striae distensae (rubrae) in monozygotic twins, *Pediatr. Dermatol.* 18 (3) (2001) 261.
- [10] S. Shuster, The cause of striae distensae, *Acta Derm. Venereol.* 59 (85) (1979) 161.
- [11] L. Poivedin, Stria gravidarum: their relation to adrenal cortical hyperfunction, *Lancet* 2 (1959) 436.
- [12] P.K. Nigam, Striae cutis distensae, *Int. J. Dermatol.* 28 (1989) 426.
- [13] Y. Shirai, Studies on striae cutis of puberty, *Hiroshima J. Med. Sci.* 8 (1959) 215.
- [14] H.M. Sheu, H.S. Yu, C.H. Chang, Mast cell degranulation and elastolysis in the early stage of striae distensae, *J. Cutan. Pathol.* 18 (6) (1991) 410.
- [15] G. Singh, L.P. Kumar, Striae distensae, *Indian J. Dermatol. Ve.* 71 (5) (2005) 370.
- [16] T. Tsuji, M. Sawabe, Elastic fibres in striae distensae, *J. Cutan. Pathol.* 15 (1988) 215.
- [17] R.E.B. Watson, E.J. Parry, J.D. Humphries, C.J.P. Jones, D.W. Polson, C.M. Kiely, C.E.M. Griffiths, Fibrillin microfibrils are reduced in skin exhibiting striae distensae, *Brit. J. Dermatol.* 138 (6) (1998) 931.
- [18] K.S. Lee, Y.J. Rho, S.I. Jang, M.H. Suh, J.Y. Song, Decreased expression of collagen and fibronectin genes in striae distensae tissue, *Clin. Exp. Dermatol.* 19 (4) (1994) 285.
- [19] C. Viennet, J. Bride, V. Armbruster, F. Aubin, A.C. Gabiot, T. Gharbi, P. Humbert, Contractile forces generated by striae distensae fibroblasts embedded in collagen lattices, *Arch. Dermatol. Res.* 297 (1) (2005) 10.
- [20] L. Olsen, J.A. Sherratt, P.K. Maini, A mechanochemical model for adult dermal wound contraction: on the permanence of the contracted tissue displacement profile, *J. Theor. Biol.* 177 (2) (1995) 113.
- [21] J.D. Murray, *Mathematical Biology: Spatial Models and Biomedical Applications*, Springer Verlag, 2003.
- [22] A.S. Hariharan, Development of striae distensae: a mechanochemical model, Master's thesis, Auburn University, 2007.
- [23] J.L. Burton, S. Shuster, A rapid increase in skin extensibility due to prednisolone, *Brit. J. Dermatol.* 89 (5) (1973) 491.
- [24] G.E. Piérard, Iatrogenic alterations of the biomechanical properties of human skin, *Brit. J. Dermatol.* 98 (1) (1978) 113.
- [25] J.L. Rinn, J.K. Wang, H. Liu, K. Montgomery, M. van de Rijn, H.Y. Chang, A systems biology approach to anatomic diversity of skin, *J. Invest. Dermatol.* 128 (4) (2008) 776.
- [26] G.F. Oster, J.D. Murray, A.K. Harris, Mechanical aspects of mesenchymal morphogenesis, *J. Embryol. Exp. Morphol.* 78 (1983) 83.
- [27] B.L. Vaughan, Jr., R.E. Baker, D.A. Kay, P.K. Maini, in preparation.
- [28] V.H. Barocas, A.G. Moon, R.T. Tranquillo, The fibroblast-populated collagen microsphere assay of cell traction forcepart 2: measurement of the cell traction parameter, *J. Biomech. Eng.* 117 (1995) 161.
- [29] D.M. Knapp, V.H. Barocas, A.G. Moon, K. Yoo, L.R. Petzold, R.T. Tranquillo, Rheology of reconstituted type I collagen gel in confined compression, *J. Rheol.* 41 (1997) 971.
- [30] A.G. Moon, R.T. Tranquillo, Fibroblast-populated collagen microsphere assay of cell traction force: Part 1. continuum model, *AIChE J.* 39 (1) (1993) 163.
- [31] G.W. Scherer, S.A. Pardenek, R.M. Swiatek, Viscoelasticity in silica gel, *J. Non-Cryst. Solids* 107 (1) (1988) 14.
- [32] D.I. Shreiber, V.H. Barocas, R.T. Tranquillo, Temporal variations in cell migration and traction during fibroblast-mediated gel compaction, *Biophys. J.* 84 (6) (2003) 4102.
- [33] P. Lehmann, P. Zheng, R.M. Lavker, A.M. Kligman, Corticosteroid atrophy in human skin. a study by light scanning and transmission electron microscopy, *J. Invest. Dermatol.* 81 (2) (1983) 169.
- [34] J.L. Leveque, J. Rigal, P.G. Agache, C. Monneur, Influence of ageing on the in vivo extensibility of human skin at a low stress, *Arch. Dermatol. Res.* 269 (2) (1980) 127.